Design of Wireless Power Transfer System for PMBLDC Motor driven Autonomous Vehicle

Phaneendra Babu Bobba[1*], *Sai Surya Vidul* Chinthamaneni[1], *Vedavyas Manjunath* D[1], *Ahmed Hussein* Alkhayyat[2], *Divya* Pandey[3]

[1]Gokaraju Rangaraju Institute of Engineering and Technology, Hyderabad, Telangana, India
[2] Computer Technical Engineering Department, College of Technical Engineering, The Islamic University, Najaf, Iraq
[3] Uttaranchal School of Computing Sciences, Uttaranchal University, Dehradun 248007 INDIA

Abstract. In the modern age of technology where everything is powered via physical wires, once considered a technical marvel has now become a bane. Wireless power transfer is the key to the future of power transfer, in this paper a 1kW WPT system is designed and simulated for an PMBLDC motor driven autonomous vehicle. This paper focuses in detail about the variation in performance of the coils and the overall system when ferrite cores and aluminum shielding is considered along with the coils. It provides a comprehensive analysis on the misalignment of transmitter and receiver coils in different orientations and distances. The results indicate a significant increase in power transfer and efficiency of the system when extra components such as cores and shielding are also implemented. It is oriented towards increasing the efficiency of powering autonomous vehicles used in various sectors such as automobiles, information technology, aerospace, robotics, precision and domestic equipment, etc.

1 Introduction

WPT is a relatively new concept but is very promising and can lead us to the future by changing the primitive way of charging electronics through physical wires. By implementing WPT we can remove the need to use wire which prohibits the implementation of an application in many ways, thus making electronics more flexible and dynamic.

Autonomous vehicles have various applications and can be implemented in many more categories of technology for simple use cases such as cargo transfer to complex cases such as the production of microprocessors at the nanometer level. This can be achieved by integrating the WPT system with such autonomous machines. This not only leads to an increase in efficiency but also reduces time and dependency on the charging of machines or to provide constant supply to applications through wires.

* Corresponding Author: bobbaphani@griet.ac.in

This combination can be implemented in any field. One such application which is widely adopted and used now is EVs. The main adversity of EVs is the charging of batteries through electric charge stations. This can be solved using a WPT system, which can be implemented according to the requirement of the EVs.

2 Designing of WPT system for autonomous vehicle

In designing a WPT system, various considerations and factors are considered according to the already established standards for wireless power transfer. The following considerations were taken account while designing the WPT system for an autonomous vehicle.

2.1 Area consideration

The area present in the autonomous vehicle considered in the project is shown in Fig 1.

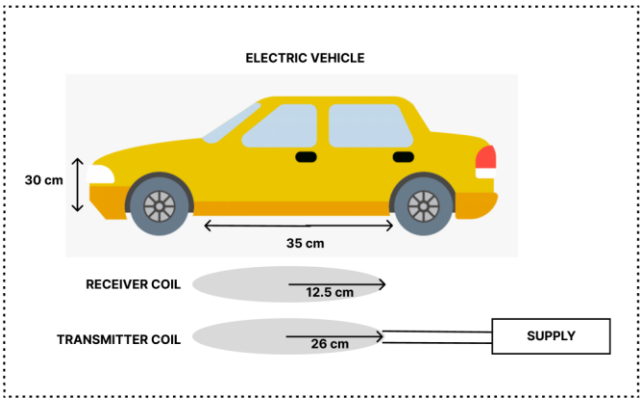

Fig 1. Block Diagram of dimensions of electric vehicle

When designing a WPT system for an electric vehicle we need to consider the area available to place the coil, the cost of material used, the dimensions of the coil required to provide the required power output, without compromising on efficiency and performance characteristics on varying loads [2]. Thus, taking into consideration all the above requirements the receiver coil is designed accordingly with a radius of 26 cm [10].

2.2 Coil design

Designing transmitter and receiver coils for a WPT system plays a vital role. The following considerations are taken into account in designing efficient coils [11].

2.2.1 Litz wire

In this project, a type 2 construction type litz wire is considered. This type of construction is widely preferred for high-frequency WPT systems. It consists of bundles of twisted type 1 litz wire. In addition, a single film coating thickness is also considered in order to reduce the diameter of the wire. Finally, an outer insulation of double nylon is used in order to protect the litz wire from external effects and insulate flux lines from coming out of the wire.

2.2.2 Number of turns

For this project a circular coil is considered with zero pitch, this makes the number of turns a crucial factor in achieving the required coupling coefficient and inductances. Formula (1) provides the number of turns to be considered for a coil.

$$N = \frac{Outer\ radius - Inner\ radius}{Thickness\ of\ the\ conductor} \quad (1)$$

This formula provides the number of turns used in transmitter and receiver considering the radius of outer and inner circles, along with thickness. Thus, providing a value more appropriate to the type of conductor used and the dimensions of the coil.

2.2.3 Inductance of coils

To design a hardware model of a WPT system. We need to calculate the self and mutual inductance of the coils, as they dictate how the flux is acting in the coil and around the coil. The formula (2) provides the self-inductance of a coil [5].

$$L(H) = \frac{N^2(D_o - N(Th))^2}{16D_o + 28N(Th)} \times \frac{39.37}{10^6} \quad (2)$$

N = Number of turns
D_o = Diameter of Outer Radius of coil
Th = Thickness of the coil

The mutual inductance of the coils is given by the following formula (3) [6].

$$M = K\sqrt{L_T L_R} \quad (3)$$

K = Coupling Coefficient
L_T = Self inductance of Transmitter coil
L_R = Self-inductance of Receiver coil

3 Block diagram

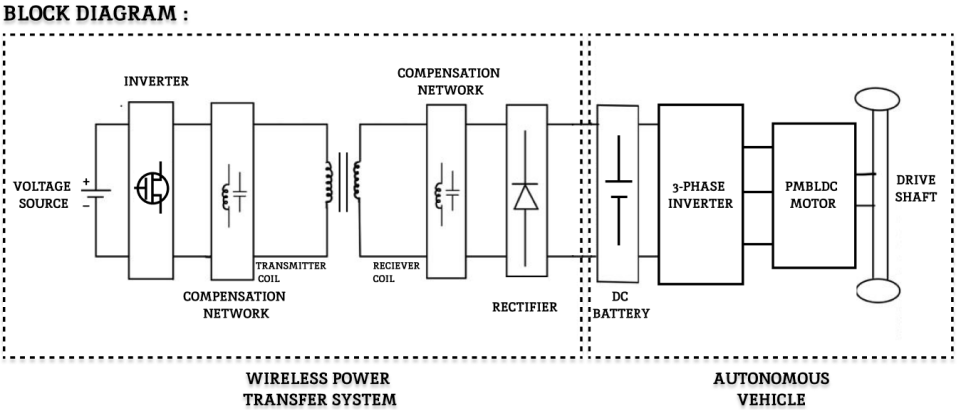

Fig. 2. Block Diagram of autonomous vehicle in combination with a WPT system

The entirety of the WPT system integrated with an autonomous vehicle can be seen in Fig 2. This block diagram can be divided and explained in two parts, wireless power transfer system and the autonomous vehicle.

3.1 Wireless power transfer system

Wireless Power Transfer System contains various components. It primarily contains a voltage source which provides the required DC output, this output is fed into a two level H bridge inverter. The inverter helps in the conversion of DC to AC supply, this supply is used to excite the transmitter (primary coil). A compensation network of series-series C type is used to match the impedance of source and load circuits [2][6], as well as help in increasing the efficiency of the system. The main aim of using series-series compensation is to tune the resonant frequency of source and load circuits.

The receiver (secondary coil) obtains voltage via the principle of mutual inductance, the obtained current is then run through a compensation network similar to the one used in the transmitter side. The stabilized output is then run through a rectifier to convert the obtained AC voltage into DC, to store the output power generated by the WPT system in a battery [6].

3.2 Autonomous vehicle

This part of the circuit contains the driving mechanism, driveshaft, DC battery and electric drive system. DC battery is used to store the output from the WPT system, thus powering the entire drive mechanism of the autonomous vehicle. The DC power obtained from the battery is then converted into 3 phase AC power where the signals are lagged by 120 degrees. The inverter is then used to power a permanent magnet BLDC motor which is the heart of the drive system, thus providing the necessary mechanical output to move the mechanical transmission of the vehicle.

4 Ansys model

Ansys finite element analysis software was used in this work to simulate computer models of structures and electronics to understand electromagnetism. Using Ansys Maxwell, a top electromagnetic field simulation tool, we can examine coil parameters such as mutual inductance, coupling coefficient, and the self-inductances of the transmitter and receiving coils. A finite element study of the coil constructions was also finished using the Ansys Maxwell software, and graphs of the magnetic field distribution were made [9]. Numerous coil configurations have been developed to compare and evaluate the efficiency, cost, and weight of wireless power transfer. Comparisons between the coil systems with ferrite cores, with ferrite cores and aluminum shielding and without any of these components have been made.

4.1 Simulation of coils without ferrite cores and aluminium shielding

The below proposed simulations are done with the considerations mentioned above, air is considered as the medium around the coil setup. Battery specification in Table 1 and coil parameters in Table 2, are considered common for all the simulations below [4][6].

Table 1. Battery specifications of autonomous vehicle

PARAMETER	VALUE
Capacity	20,000 mAh
Voltage	48V
Power	1KW

Table 2. Coil parameters

PARAMETER	TRANSMITTER	RECEIVER
Rout	260mm	125mm
Rin	87mm	41.6mm
Current	25A	20A
Turns	28	17
Thickness of coil	6 AWG	8 AWG
Distance between coils	100mm	

Fig 3 displays the simulation of the coils placed in a core-less medium with the surrounding environment being air. This simulation is done with a distance of 100mm between the transmitter and receiver [9].

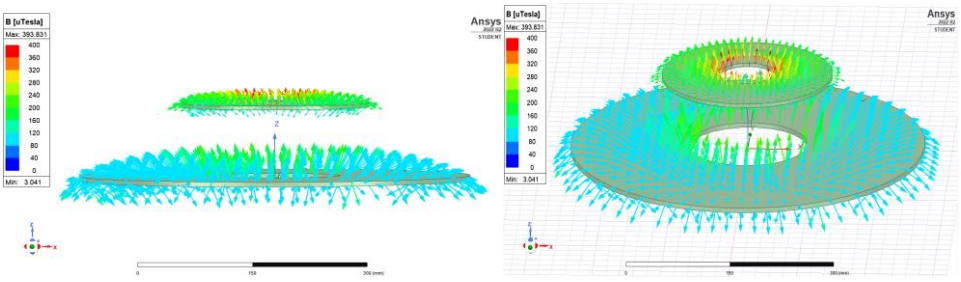

(a) **(b)**

Fig 3. Simulation of coils without ferrite core; (a) Horizontal view of coils; (b) Vertical view of coils

Table 3 represents the ansys output results obtained from the simulation of the coils without cores and shielding. The results depict the self-inductances, coupling coefficient and mutual inductance values of the coils. A coupling coefficient of 0.199 indicates efficient coupling and flux linkage between the coils.

Table 3. Ansys output for without cores and shielding case

PARAMETER	**VALUE**
Frequency	85 kHz
Coupling Coefficient of each coil	1.0000
Coupling Coefficient between both coils	0.199
Transmitter Inductance	0.293 mH
Receiver Inductance	0.047 mH
Mutual Inductance	0.022 mH

4.2 Simulation of coils with ferrite

Table 4 represents the input coil parameters used for the simulation of coils along with the implementation of ferrite cores of 2mm thickness [3][4][8].

Table 4. Coil parameters

PARAMETER	**TRANSMITTER**	**RECEIVER**
Rout	260mm	125mm
Rin	87mm	41.6mm
Current	25A	20A
Turns	28	17
Thickness of coil	6 AWG	8 AWG
Distance between coils	100mm	
Thickness of Ferrite core	2mm	

Fig 4 represents the simulation of coils which are placed along with a ferrite core of 2mm on both coils. This simulation is done with 100mm between the transmitter and receiver. It displays the linkage of flux lines and represents the magnetic vector lines inside and between the coils [9].

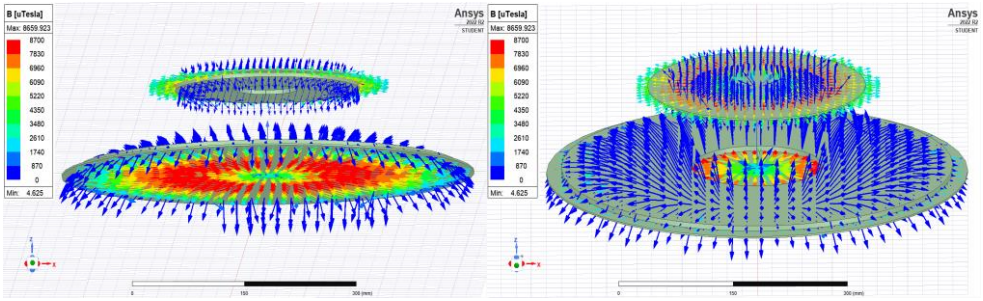

(a) **(b)**

Fig 4. Simulation of coils with ferrite core; (a) Horizontal view of coils; (b) Vertical view of coils

Table 5 represents the ansys output for the simulation of coils with ferrite cores on both the plates. From the results it can be concluded that, the coupling coefficient increased to 0.265 from 0.199. The self-inductances and mutual inductances values also have an increase in value, indicating an overall increase in coil performance.

Table 5. Ansys output for simulation of coils with ferrite cores

PARAMETER	**VALUE**
Frequency	85 kHz
Coupling Coefficient of each coil	1.0000
Coupling Coefficient between both coils	0.265
Transmitter Inductance	0.473 mH
Receiver Inductance	0.087 mH
Mutual Inductance	0.054 mH

4.3 Simulation of coils with ferrite cores and aluminium shielding

Table 6 represents the input coil parameters considered for the simulation of the coils which are placed along with a ferrite cores and aluminium shielding on both the coils. This simulation is done with a distance of 100mm between the transmitter and receiver. The following parameters are considered for the simulation [3][4][8].

Table 6. Coil parameters

PARAMETER	**TRANSMITTER**	**RECEIVER**
Rout	260mm	125mm
Rin	87mm	41.6mm
Current	25A	20A
Turns	28	17
Thickness of coil	6 AWG	8 AWG
Distance between coils	100mm	
Thickness of Ferrite core	2mm	
Thickness of Aluminium shielding	2mm	

The simulation of coils along with ferrite cores and aluminium shielding can be seen in Fig 5. It depicts the magnetic profile and linkage of flux of coils when cores and shielding is considered.

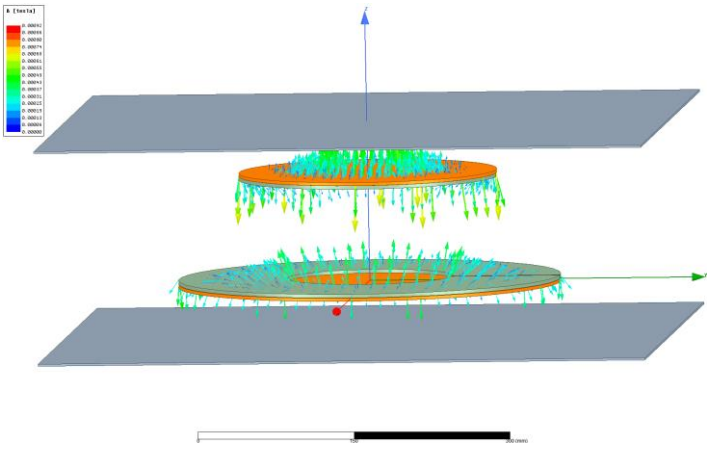

Fig 5. Simulation of coils with ferrite core and aluminium shielding

Table 7 depicts the results obtained from the ansys simulation of coils with ferrite cores and aluminium shielding. From the results it can be concluded that there is a marginal decrease in coupling coefficient from 0.265 to 0.227, but mainly provides protection from external factors in affecting the coil operation.

Table 7. Ansys output for simulation of coils with ferrite cores and aluminium shielding

PARAMETER	**VALUE**
Frequency	85 kHz
Coupling Coefficient between both coils	0.227
Transmitter Inductance	0.366 mH
Receiver Inductance	0.080 mH
Mutual Inductance	0.038 mH

4.4 Comparative analysis

Table 8 represents the comparison of results obtained in the three cases mentioned above.

Table 8. Comparison of results

Parameter	**Coils**	**Coupling coefficient**	**Inductances**	**Mutual inducantces**
Without ferrite cores and aluminium shielding	Transmitter	0.199	0.293 mH	0.022 mH
	Receiver		0.047 mH	
With ferrite cores	Transmitter	0.265	0.473 mH	0.054 mH
	Receiver		0.087 mH	
With ferrite cores and aluminium shielding	Transmitter	0.227	0.366 mH	0.038 mH
	Receiver		0.080 mH	

The above highlights a major increase in all the parameters when a ferrite core is used. The ferrite core also helps in keeping the flux lines concentrated within the coils. This shows that a simple ferrite core helps in increasing efficiency and most importantly the coupling coefficient between the coils indicating good power transfer.

The above study represents how ferrite cores and aluminium shielding effect the inductance values of the coils drastically. In the case of no cores and shielding, the coil performs poorly, with less mutual inductance and coupling coefficient values when compared to the other two cases. In the case of coils with ferrite cores, it increases the inductance and coupling coefficient values drastically, but some residual flux is lost to the surrounding environment [3]. In order to solve this issue, we consider the coil along with ferrite cores and aluminium shielding. The aluminium shielding helps in stopping the escape of flux and provides

protection from the outside environment to the coils. The implementation of aluminium shielding is also very easy and cost effective, making it preferable for such WPT applications.

4.5 Misalignment of coils in different orientations

Misalignment of transmitter and receiver is common in WPT systems, as often there might be a small misalignment of coils irrespective of perfect positioning. In order to understand the changes in inductance and coupling coefficient values, in this project misalignment cases in the X, Y, and Z directions are considered. The below Fig 6 displays the simulations done at a distance of 25mm, 50mm and 75mm in X direction, 25mm in Y directions and 150mm in Z direction, from the actual position.

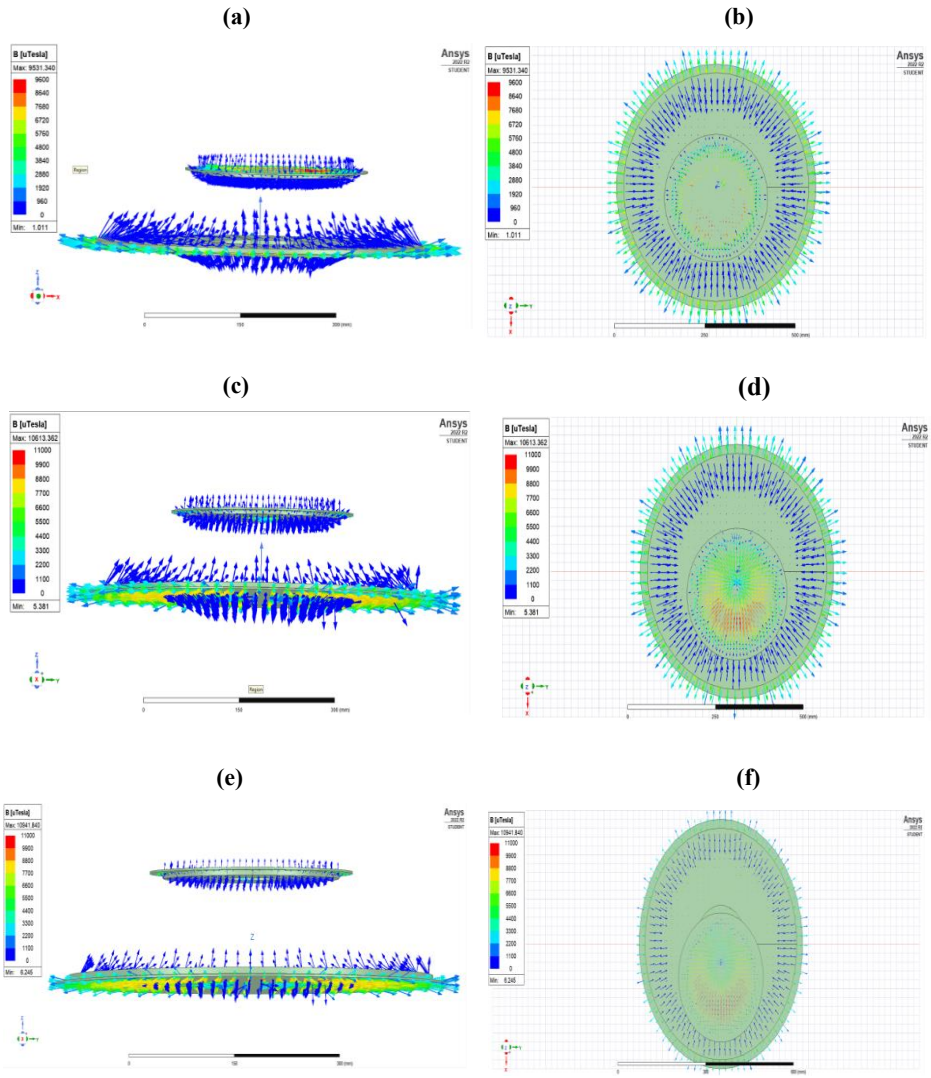

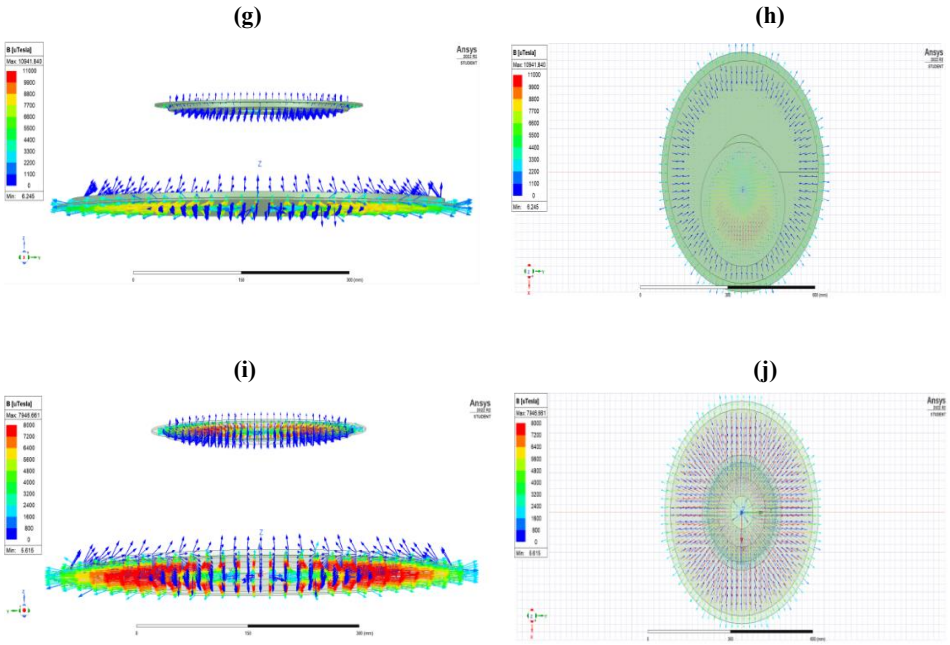

Fig 6. Simulation of coils with ferrite core and aluminium shielding; (a) Horizontal view misalignment in X-axis by 25mm; (b) Top view misalignment in X-axis by 25mm; (c) Horizontal view misalignment in X-axis by 50mm; (d) Top view misalignment in X-axis by 50mm; (e) Horizontal view misalignment in X-axis by 75mm; (f) Top view misalignment in X-axis by 75mm; (g) Horizontal view misalignment in Y-axis by 25mm; (h) Top view Misalignment in Y-axis by 25mm; (i) Horizontal view misalignment in Z-axis by 150mm; (j) Top view misalignment in Z-axis by 150mm

The misalignment displayed in Fig 6, showcase how the coils are positioned when they are placed away from the actual position at different distances. It shows how the flux linkage decreases between the coils, causing a decrease in coupling coefficient as the distance from the actual position increases.

4.6 Misalignment analysis

Table 9. Misalignment output

PARAMETERS	L(Transmitter)	L(Receiver)	Mutual Inductance	Coupling Coefficient
X-25mm	0.474 mH	0.088 mH	0.053 mH	0.262
X-50mm	0.477 mH	0.088 mH	0.050 mH	0.247
X-75mm	0.481 mH	0.088 mH	0.046 mH	0.226
Y-25mm	0.474 mH	0.088 mH	0.053 mH	0.261
Z-150mm	0.468 mH	0.085 mH	0.033 mH	0.164

Thus, considering all the above misalignment cases, here below is the comparison of the cases considered. The above table clearly depicts the change in inductances of the coil, mutual inductances and coupling coefficients. As the inductances of the coil relatively stay similar, we can observe a major change in mutual inductances and coupling coefficients. As the misalignment increases from 25mm gradually to 75mm on X-axis the mutual inductance between the coils and coupling coefficient gradually decreases from 0.262 to 0.226. Misalignment in Y-axis also provides similar output as its counterpart in the X-axis simulation. Finally, the misalignment case in the Z-axis is done only to understand the change in values of parameters, but in a practical approach as the distance between the transmitter and receiver are fixed this case is not possible. It can be observed that an increase in distance between the coils in Z-axis leads to a drastic drop in all parameters, indicating weak flux linkage between the coils.

5 LT spice model

LT Spice is a software based on analog electronic circuit simulation software used for analysing electrical circuits to obtain power, voltage and current characteristics at different terminals of the circuit. The efficiency of the coil structures designed can be obtained using this software. An LT spice model is built to simulate and understand the working of the WPT system as whole. In order to understand how the WPT system works in different conditions, two models are considered, without cores and shielding and a case with cores and shielding.

5.1 LT spice model for only coils

In this scenario ferrite cores and aluminium shielding are not considered. Thus, the model is simulated in accordance with those inductance values as seen above. The compensation is tuned in order to achieve higher efficiency. Table 10 represents the input parameters are considered in this model.

Table 10. Model parameters

PARAMETER	**VALUE**
Input Voltage	190V
Input Current	26.8 A
Transmitter side Capacitance	19.08nF
Receiver side Capacitance	73.99nF
Transmitter Inductance	0.293 mH
Receiver Inductance	0.047 mH
Mutual Inductance	0.022 mH
Input Power	1.2683 KW
Frequency	85KHz

The LT spice schematic used to model the system can be seen in Fig 7. The schematic is built using T model, where the mutual inductance is considered as an inductor between the trasnmitter and reciever inductors in the schematic.

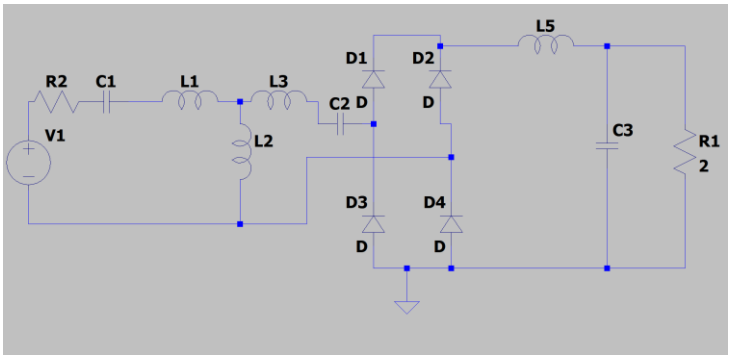

Fig 7. LT spice schematic

Input voltage and current waveforms considered across the input voltage supply can be seen in Fig 8. Where the black signal represents voltage and blue signal represents current.

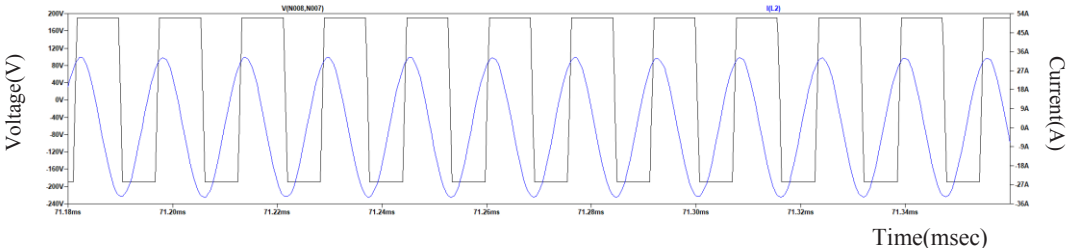

Fig 8. Input voltage and current waveform

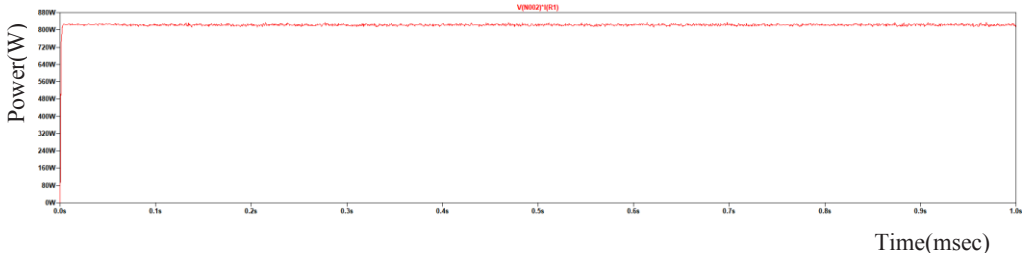

Fig 9. Output power waveform

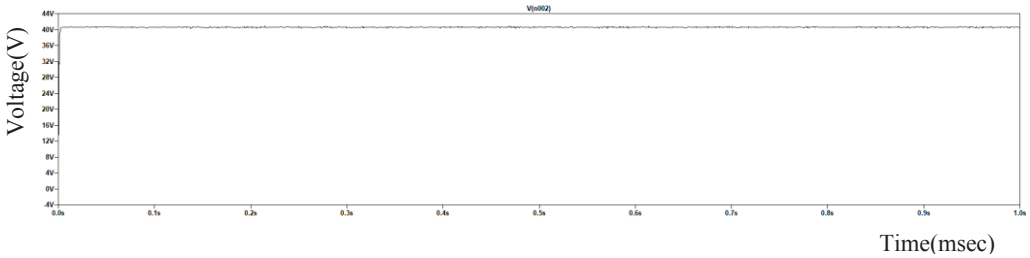

Fig 10. Output voltage waveform

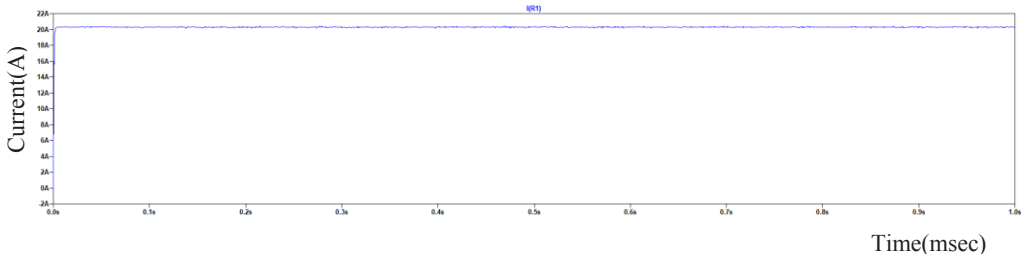

Fig 11. Output current waveform

The output power, voltage and current waveforms obtained from the simulation of model can be seen in Fig 9 to 11. The specific values can be seen in Table 11. The efficiency of the system is 64.8% which can be considered low.

Table 11. LT spice model results

PARAMETER	**VALUE**
Output Voltage	41V
Output Current	20.805A
Output Power	822 W
Efficiency	64.8%

5.2 LT SPICE MODEL FOR COIL WITH FERRITE CORES AND ALUMINIUM SHEILDING

In this model ferrite cores and aluminium shielding are considered while designing the model. The main difference between the two cases is in the inductance values, weight of the model and material used. Table 12 represents the input parameters are considered in this model.

Table 12. Model parameters

PARAMETER	**VALUE**
Input Voltage	190V
Input Current	17.74A
Transmitter side Capacitance	26.78nF
Receiver side Capacitance	49.19nF
Transmitter Inductance	366.363 uH
Receiver Inductance	80.024 uH

Mutual Inductance	38.889 uH
Input Power	1.2683KW
Frequency	85KHz

The schematic shown in Fig 7 is considered to be the same in the simulation of this case. The only difference being the input parameters from Table 12 are considered in this simulation. The input voltage and current waveforms can be seen in Fig 12. Where the black signal represents voltage and blue signal represents current.

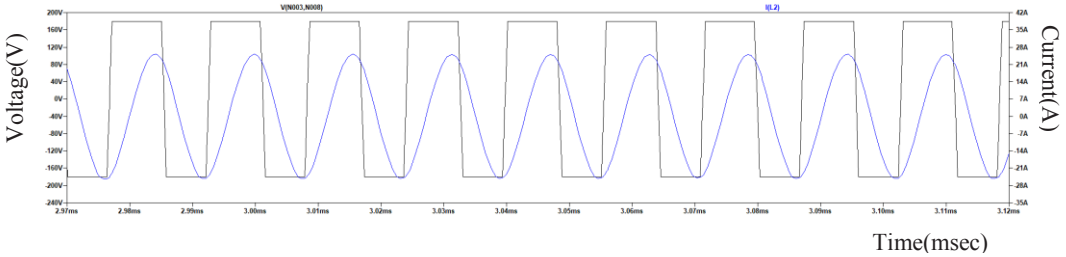

Fig 12. Input voltage and current waveform

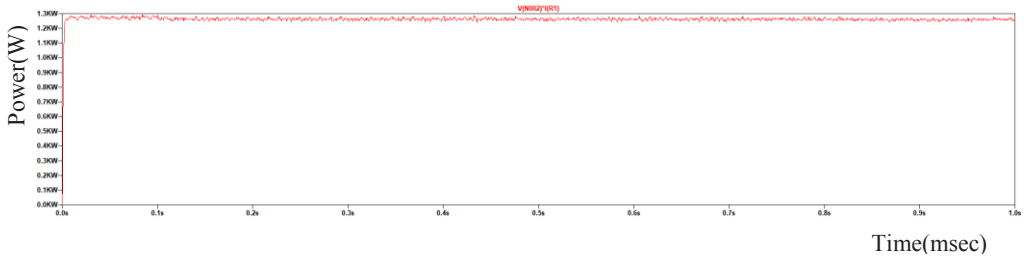

Fig 13. Output power waveform

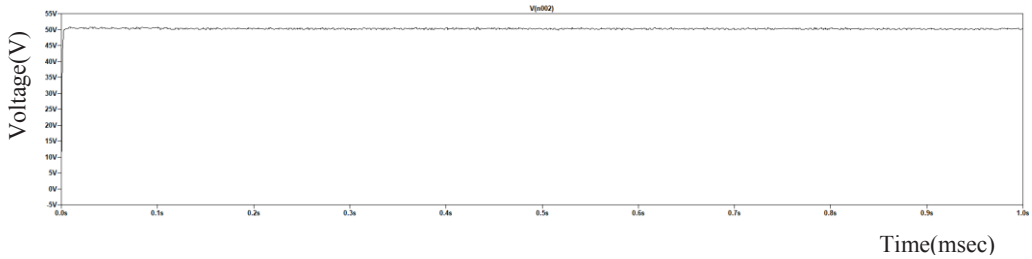

Fig 14. Output voltage waveform

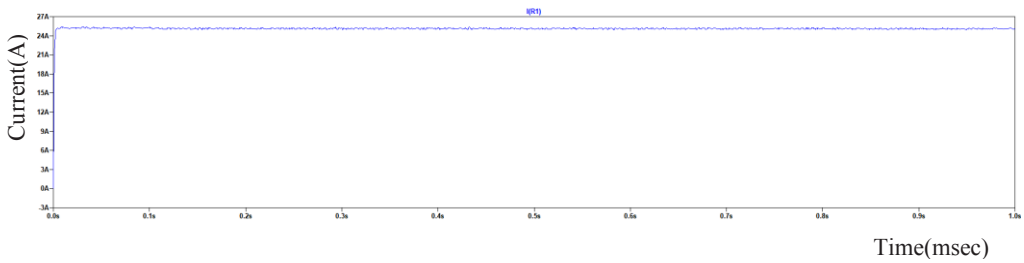

Fig 15. Output current waveform

The output power, voltage and current waveforms obtained from the simulation of model can be seen in Fig 13 to 15. The specific values can be seen in Table 13. The efficiency of the system is 98.5% which can be considered a good standard.

Table 13. LT spice model results

PARAMETER	VALUE
Output Voltage	50.232V
Output Current	25.116A
Output Power	1.25KW
Efficiency	98.5%

5.3 Comparative study

Table 14. Comparison of results

Coil design	Power Transmitter	Power Receiver	Efficiency
Coil without ferrite	1.26KW	822W	64.8%
Coil with ferrite cores and aluminium shielding	1.26KW	1.25KW	98.5%

The above Table 14 reflects the drastic improvement in efficiency and power transfer between coils when cores and shielding is considered. When cores and shielding are considered, the efficiency jumps from 64.8% to 98.5%, this shows how well the cores help in increasing of flux linkage and how the shielding stops any loss of flux to the surroundings. Therefore, to increase the overall efficiency of the system we can utilize cores and shielding as they are a cost effective and easy to implement .

6 Conclusion

In this paper a wireless power transfer system is designed and simulated for a PMBLDC motor driven autonomous vehicle of 48V battery with a capacity of 20,000mAh, a transfer of 1kW is achieved. A detailed analysis is showcased on how external components such as ferrite cores and aluminium shielding effect the coupling of flux between the coils. The Ansys results indicate drastic improvement in performance and efficiency of coils when ferrite cores and aluminium shielding are considered. Misalignment analysis is also depicted in detail for X,Y and Z directions, where parameters such as self-inductances, mutual inductance, coupling coefficient decrease as the distance increases. This also causes an increase in losses of coils. An overall system is designed and simulated using LT spice for two cases, only coils

and coils along with ferrite cores and aluminium shielding. The efficiency of the system has increased significantly from 64.8% to 98.5%.

References

1. Charles R. Sullivan, Richard Y. Zhang, Simplified Design Method for Litz Wire, IEEE, (2014).
2. Siqi Li, and Chunting Chris Mi, Wireless Power Transfer for Electric Vehicle Applications, IEEE (2013).
3. Linlin Tan, Kamal Eldin Idris Elnail, Minghao Ju and Xueliang Huang, Comparative Analysis and Design of the Shielding Techniques in WPT Systems for Charging EVs, Energies, (2019).
4. Nagarjuna, A., Suresh Kumar, T., Yogeswara Reddy, B., Udaykiran, M., Fifteen level cascaded H-bridge multilevel inverter fed induction motor, International Journal of Innovative Technology and Exploring Engineering, 2019, 8(11), pp. 640–645.
5. New England Litz Wire Specifications
6. Mahalle, G., Kotkunde, N., Gupta, A.K. et al. Microstructure Characteristics and Comparative Analysis of Constitutive Models for Flow Stress Prediction of Inconel 718 Alloy. J. of Materi Eng and Perform 28, 3320–3331 (2019).
7. Benjamin H. Waters, Brody J. Mahoney, Gunbok Lee and Joshua R. Smith, Optimal Coil Size Ratios for Wireless Power Transfer Applications, IEEE, (2014).
8. Tasnime Bouanou, Hassan El Fadil, Abdellah Lassioui, Ouidad Assaddiki and Sara Njili, Analysis of Coil Parameters and Comparison of Circular, Rectangular, and Hexagonal Coils Used in WPT System for Electric Vehicle Charging, World Electric Vehicle Journal, (2021)
9. Zhen Zhang, Hongliang Pang, Apostolos Georgiadis, and Carlo Cecati, Wireless Power Transfer – An Overview, IEEE, (2018)
10. Davide De Marco, Alberto Dolara , Michela Longo and Wahiba Yaïci, Design and Performance Analysis of Pads for Dynamic Wireless Charging of EVs using the Finite Element Method, Energies, (2019).
11. Naik, R.B., Ratna, D., Singh, S.K., Synthesis and characterization of novel hyperbranched alkyd and isocyanate trimer based high solid polyurethane coatings, Progress in Organic Coatings, 2014, 77(2), pp. 369–379
12. Karthik Rao, R., Bobba, P.B., Suresh Kumar, T., Kosaraju, S., Feasibility analysis of different conducting and insulation materials used in laminated busbars, Materials Today: Proceedings, 2019, 26, pp. 3085–3089.
13. Ran Chang, Li Quan, Xiaoyong Zhu, Zaiyun Zong, Huawei Zhou, Design of a Wireless Power Transfer System for EV Application Based on Finite Element Analysis and MATLAB Simulation, IEEE, (2014).
14. Tummala, S.K., Indira Priyadarshini, T., Morphological Operations and Histogram Analysis of SEM Images using Python, Indian Journal of Engineering and Materials Sciences, 2022, 29(6), pp. 794–798.
15. J.P.K. Sampath, A. Alphones, Hitoshi Shimasaki, Coil design Guidelines for High Efficiency of Wireless Power Transfer (WPT), IEEE, (2016)
16. Giuseppe Buja, Manuele Bertoluzzo, and Kishore N. Mude, Design and Experimentation of WPT Charger for Electric City-Car, IEEE TRANSACTIONS ON INDUSTRIAL ELECTRONICS, (2015).
17. Prasad, K.S., Gupta, A.K., Singh, Y., Singh, S.K., A Modified Mechanical Threshold Stress Constitutive Model for Austenitic Stainless Steels, Journal of Materials Engineering and Performance, 2016, 25(12), pp. 5411–5423

18. Raju, N.A., Suresh Kumar, T., Forward converter based switch mode power supply with modified boost converter as PFC, International Journal of Innovative Technology and Exploring Engineering, 2019, 8(11), pp. 3860–3864.
19. Kosaraju, S., Anne, V.G. & Popuri, B.B. Online tool condition monitoring in turning titanium (grade 5) using acoustic emission: modeling. Int J Adv Manuf Technol 67, 1947–1954 (2013).
20. Sandeep Pandre, Ayush Morchhale, Nitin Kotkunde & Swadesh Kumar Singh (2020) Influence of processing temperature on formability of thin-rolled DP590 steel sheet, Materials and Manufacturing Processes, 35:8, 901-909